DO-TH 93/21
OHSTPY-HEP-T-93-011
September 1993

B-MESON INCLUSIVE SEMILEPTONIC DECAY DISTRIBUTIONS IN THE PARTON MODEL

C. H. Jin[a1], W. F. Palmer[b2] and E. A. Paschos[a1]

[a]Institut für Physik
Universität Dortmund
D-44221 Dortmund, Germany

[b]Department of Physics, The Ohio State University
Columbus, Ohio 43210, USA

Abstract

The parton model for semileptonic B meson decays is studied with special attention to the decay distributions. We find that the spectra show dramatic variations when we introduce cuts on the hadronic energy or invariant mass of hadrons. Results for both $b \to u$ and $b \to c$ decays are presented. The detailed spectra may help to separate the two types of decays.

[1]Supported by Bundesministerium für Forschung und Technologie, 05-6DO93P, Bonn, FRG

[2]Supported in part by the US Department of Energy under contract DOE/ER/01545-605

DO-TH-93-21

Fermilab Library
0 1160 0027625 7

1 INTRODUCTION

The decays of B-mesons have been studied extensively and have been very useful in extracting properties of the weak interactions. In particular, the $b \to u$ transition is still an active field of investigation. On the experimental side there is a large effort hindered by the difficulty of identifying the decays of B-mesons to light quarks. This difficulty of identifying $b \to u$ events forced investigators to concentrate on the end-point spectrum of the electron energy or study exclusive decays[1]. In this article we present an extended study of the semileptonic B-decays. We are interested in the decay

$$B \to X_u + e^- \bar{\nu} \tag{1}$$

for which we wish to give explicit distributions in several kinematic variables. With the decay spectrum completely determined by a single fragmentation parameter, it may be compared to the competing process in $B \to X_c + e^- \bar{\nu}$. With the help of these distributions it should be possible to test characteristics of the decay products with various kinematical cuts, and, in particular, collect events typical for this process. The hope is that with the results presented here the experimental analyses could incorporate many more events than those confined to the endpoint region of the electron spectrum.

The first issue is the model that should be used. There are two models for the inclusive decays of reaction (1). The early model of Altarelli et al. [2], to be denoted as ACM, uses a spectator model and a distribution of quarks within the B-meson described by the Fermi motion of the spectator quark. This approach treats the phase space effects correctly, but is rather crude, as the authors state[2], because it depends on an unknown distribution function for the spectator quark. The model pictures the overall decay as the disintegration of the B-meson into the spectator quark plus the decay products of the heavy quark.

The second approach[3] uses the parton model at an infinite momentum frame (IMF). It pictures the mesonic decay as the decay of the partons. The probability of finding a b-quark in a B-meson carrying a fraction x of the mesons momentum in the IMF is given by the distribution function $f(x)$. The distribution function $f(x)$ will be identified, later on, with the observed fragmentation function of a b-quark into a B-meson. The kinematics for the

decay of a heavy to a light quark involve the correlation of two currents at short distances, where the incoherence of the decay products is justified. The decay kinematics are also different from those in deep inelastic scattering and the energy-momentum conserving δ-function has now two roots. As a result, there are two scaling variables

$$x_{\pm} = \frac{q_0 \pm |\vec{q}|}{M_B} = \frac{q_{\pm}}{M_B} \tag{2}$$

which are the light-cone variables of the current-momentum. Thus we have again scaling of the distribution function but now in terms of two variables.

In this article we compute in the parton model double- and triple-differential deay rates. As convenient variables we select the energy of the electron, E_e, and a second variable characterizing the hadronic system. The second variable is either the energy of hadron $E_X = M_B - q_0$, or the invariant mass M_X of the hadrons. For fixed q_0 or M_X, the distributions in E_e vary considerably and favor the ranges $0.5M_B \leq q_0 \leq 0.8M_B$ and $0.1M_B \leq M_X \leq 0.3M_B$ (Figs. 4 and 7).

The inclusive decays involve a three-body phase space, which is described explicitly in the next section. Special attention is paid to the boundaries of phase space because they determine the ranges of several integrations.

The plan of the paper is the following. Section 2 contains a detailed discussion of the phase space for the $B \to X_u + e^-\bar{\nu}$ channel and defines the ranges of integrations. The same discussion can be adapted for the $B \to X_c + e^-\bar{\nu}$ decay. In section 3 we discuss the model and give in equation (35) the triple differential decay rate, which can be used to fulfil the specific experimental conditions. In section 4 we display many decay spectra, for both $b \to u$ and $b \to c$ semileptonic decays and compare them with the ACM model. In section 5 we report our summary and conclusions.

2 KINEMATICS AND PHASE SPACE

The semileptonic decay is shown in Fig. 1. We define the kinematic variables:

P_B	: momentum of B-meson
P_e	: momentum of electron
P_ν	: momentum of neutrino
P_X	: momentum of hadrons
$q = P_e + P_\nu$	: momentum of current
θ	: opening angle between the electron and neutrino in the rest frame of the B-meson

From momentum conservation, we have

$$P_X = P_B - q, \tag{3}$$

or

$$M_X^2 = M_B^2 - 2M_B(E_e + E_\nu) + q^2. \tag{4}$$

Expressing q^2 as

$$q^2 = 2E_eE_\nu(1 - \cos\theta) \tag{5}$$

it follows that

$$q^2 \leq 4E_eE_\nu \tag{6}$$

for $\theta = \pi$, and

$$-2 \leq \cos\theta - 1 = \frac{M_B^2 - M_X^2 - 2M_B(E_e + E_\nu)}{2E_eE_\nu} \leq 0. \tag{7}$$

The upper limit in (7) gives

$$\frac{M_B^2 - M_X^2}{2M_B} \leq E_e + E_\nu \tag{8}$$

with the equality attained for $\theta = 0$. The lower limit, corresponding to $\theta = \pi$, gives

$$M_X^2 \leq 4(E_e - \frac{M_B}{2})(E_\nu - \frac{M_B}{2}) \tag{9}$$

which gives E_e,$E_\nu \leq M_B/2$. In what follows we specialize to $b \to u$ decays and neglect the pion mass in the minimum value of M_X^2.

We determine next the range for the invariant mass. We substitute

$$E_\nu = \frac{q^2}{2E_e(1 - \cos\theta)} \tag{10}$$

into eq. (4)

$$s = M_X^2 = M_B^2 + q^2 - 2M_B E_e - \frac{M_B q^2}{E_e(1-\cos\theta)}, \tag{11}$$

and obtain the boundaries

$$s \leq (M_B - 2E_e)(M_B - \frac{q^2}{2E_e}) \tag{12}$$

attained at $\theta = \pi$. For $s = 0$ and $\theta = \pi$ eq. (11) gives the two boundaries $q^2 = 2M_B E_e$ and $E_e = M_B/2$ shown in Fig. 2. For larger values of s the boundaries are shown by the dashed curves. By this and similar methods we arrive at the phase space corresponding to the various orders of integration.

Case A: Once we specify E_e in the range

$$0 \leq E_e \leq M_B/2, \tag{13}$$

then q^2 is limited to the range

$$0 \leq q^2 \leq 4E_e E_\nu \leq 2M_B E_e. \tag{14}$$

Finally for definite value of E_e and q^2, the range of s is

$$0 \leq s \leq (M_B - 2E_e)(M_B - q^2/2E_e). \tag{15}$$

The lower bound for s corresponds to the production of a single pion and is appropriate for the $b \to u$ decay. This approximation does not hold for the $b \to c$ decay where $s_{min} = M_D^2$.

Case B: For a definite value of $s = M_X^2$ the regions of q^2 and E_e are limited by the diagram in Fig. 2 to be

$$0 \leq s \leq M_B^2, \tag{16}$$

$$0 \leq E_e \leq \frac{M_B}{2} - \frac{s}{2M_B}, \tag{17}$$

$$0 \leq q^2 \leq 2E_e(M_B + \frac{s}{2E_e - M_B}). \tag{18}$$

These are the boundaries for the case, where the order of integrations is first over q^2, then over E_e and finally over s.

Alternatively, we can choose as variables E_e, q^2, q_0 and we discuss again two cases depending on the orders of integrations. The physical region is shown in Fig. 3.

Case C:

$$0 \leq E_e \leq M_B/2, \tag{19}$$

$$0 \leq q^2 \leq 2M_B E_e, \tag{20}$$

and

$$E_e + \frac{q^2}{4E_e} \leq q_0 \leq \frac{M_B^2 + q^2}{2M_B}. \tag{21}$$

Case D:

$$0 \leq E_e \leq M_B/2, \tag{22}$$

$$0 \leq q^2 \leq 4E_e(q_0 - E_e) \; for \; E_e \leq q_0 \leq M_B/2, \tag{23}$$

and

$$M_B(2q_0 - M_B) \leq q^2 \leq 4E_e(q_0 - E_e) \; for \; M_B/2 \leq q_0 \leq E_e + M_B/2. \tag{24}$$

This completes the discussion for the kinematics of the decay $b \to u$. There are similar considerations for the decay $b \to c$, which modify the numerical values for the boundaries. The calculation is straight forward and we do not discuss it in detail. In section 4 we shall show the difference in the spectra with the smaller boundaries for $b \to c$ which should help to separate the two decay modes.

3 THE MODEL

The model was already described in articles [3, 4] where several spectra were also computed. Here we repeat several of the steps in order to point out new features. The decay is in general defined as

$$d\Gamma = \frac{G^2 |V_{ub}|^2}{(2\pi)^5 M_B} L^{\mu\nu} W_{\mu\nu} \frac{d^3P_e}{2E_e} \frac{d^3P_\nu}{2E_\nu}. \tag{25}$$

The leptonic tensor has the simple form

$$L^{\mu\nu} = 2(P_e^\mu P_\nu^\nu + P_\nu^\mu P_e^\nu - g^{\mu\nu} P_e \cdot P_\nu + i\varepsilon^{\mu\nu}{}_{\alpha\beta} P_e^\alpha P_\nu^\beta). \tag{26}$$

The hadronic tensor is defined in analogy to deep inelastic scattering

$$W_{\mu\nu}(P_B, q) = -g_{\mu\nu} W_1(q^2, q\cdot P_B) + \frac{P_{B\mu} P_{B\nu}}{M_B^2} W_2(q^2, q\cdot P_B) - i\varepsilon_{\mu\nu\alpha\beta} \frac{P_B^\alpha q^\beta}{M_B^2} W_3(q^2, q\cdot P_B) + \cdots \tag{27}$$

where the integration over the hadronic variables was already carried out. The structure functions $W_i(q^2, q\cdot P_B)$ contain the structure of the B-meson. The model pictures the decay as the decay of a free quark times the probability $f(x)$ of finding the quark with momentum xP_B within the B-meson. In the model

$$W_1(q^2, q\cdot P_B) = 4\int dx f(x) \delta(x^2 P_B^2 - 2xq\cdot P_B + q^2)(xP_B^2 - q\cdot P_B), \tag{28}$$

$$W_2(q^2, q\cdot P_B)/M_B^2 = 8\int dx f(x) \delta(x^2 P_B^2 - 2xq\cdot P_B + q^2) x, \tag{29}$$

$$W_3(q^2, q\cdot P_B)/M_B^2 = -4\int dx f(x) \delta(x^2 P_B^2 - 2xq\cdot P_B + q^2). \tag{30}$$

The δ-function indicates the decay of a b-quark with momentum xP_B to massless quarks. The δ-function has two roots and is simplified to

$$\delta(x^2 P_B^2 - 2xq\cdot P_B + q^2) = \frac{1}{2M_B |\vec{q}|}[\delta(x - x_+) + \delta(x - x_-)]. \tag{31}$$

with $x_\pm = (q_0 \pm |\vec{q}|)/M_B = q_\pm/M_B$. One difference from deep inelastic scattering is the existence of two roots, that is to say of two scaling variables. After carrying the integrations over x we arrive at the structure functions[3]

$$W_1(q^2, q\cdot P_B) = 2[f(x_+) - f(x_-)], \tag{32}$$

$$W_2(q^2, q\cdot P_B)/M_B^2 = \frac{4}{M_B |\vec{q}|}[x_+ f(x_+) + x_- f(x_-)], \tag{33}$$

$$W_3(q^2, q\cdot P_B)/M_B^2 = -\frac{2}{M_B |\vec{q}|}[f(x_+) + f(x_-)]. \tag{34}$$

[3]Note that the structure functions in the present article are different from those in [4].

Substituting the W_i's in eq. (25) we arrive at the triple differential decay rate

$$\frac{d\Gamma}{dE_e dq^2 ds} = \frac{G^2 |V_{ub}|^2}{8\pi^3 M_B} \frac{q_0 - E_e}{|\vec{q}|} \{x_+ f(x_+)(2E_e - M_B x_-) + (x_+ \leftrightarrow x_-)\}. \tag{35}$$

This formula is simple and shows the dependence on the two light-cone variables $x_\pm$.

The distribution function $f(x)$ is in principle unknown, but there are physical arguments[3, 5, 6] relating it with the fragmentation function of a b-quark producing a B-meson. The fragmentation function was measured in several experiments and can be represented[6, 7] as

$$f(x) = N \frac{x(1-x)^2}{[(1-x)^2 + \varepsilon_p x]^2} \tag{36}$$

with ε_p a parameter and N the normalization factor. We will use three values

$$\varepsilon_p = \begin{matrix} 0.003 \\ 0.006 \\ 0.009 \end{matrix} \tag{37}$$

with corresponding normalization factors

$$N = \begin{matrix} 0.09 \\ 0.13 \\ 0.17 \end{matrix} . \tag{38}$$

Finally, we must comment on the kinematic regions where the model is valid. Two criteria must be fulfilled.

(i) The decay involves the correlation of two currents. We are more confident in applying the model when this distance between the two currents is close to the light-cone or at short distances.

(ii) The model should apply in the region where many particles are produced. Thus, we must avoid the edge of the phase space where one or two

pions are produced. These are the lines ab and bc in Fig. 2. An additional motivation for avoiding these regions is the following. In calculating the decay distributions we used quark kinematics in an infinite momentum frame. For the phase space, however, we used the kinematics of the physical particles. At the edges of the phase space these two procedures are not always consistent with each other and may lead to contradictions.

To sum up, we feel rather confident in using the parton model for the decay $B \to X_u + e^-\bar{\nu}$ away from the edges of the phase space. For the decay $B \to X_c + e^-\bar{\nu}$, we are less confident, because the distances involved are larger. However, we also present results for this mode in section 4 which show some crucial differences between the two decays.

4 DECAY SPECTRA

As we mentioned, one of the purposes of this work is to present detailed spectra which can eventually be compared with experiments. The simplest parameter to measure is the electron energy. In addition one may be able to measure the total hadronic energy $E_X = M_B - q_0$. In Fig. 4 we show the double differential decay rate in E_e and q_0. The spectra show a striking dependence of q_0. Most of the events occur for $0.3M_B \leq E_X \leq 0.5M_B$. For smaller hadronic energies the spectra shift to higher electron energies, $E_e \geq 2.0\ GeV$. This correlation of events may help to isolate $b \to u$ events.

The integrated spectrum $d\Gamma/dE_e$ is shown in Fig. 5 for three fragmentation parameters ε_p. In the same figure we show the corresponding spectra for $b \to c$, to which we return later on. For comparison we calculated the spectrum $d\Gamma/dE_e$ in the ACM model[2]. We show in Fig. 6 the ACM and parton spectra together. In these spectra we include QCD radiative corrections which appear as a multiplicative factor. Specifically the uncorrected, $d\Gamma^{(0)}/dE_e$, and the final widths are given as

$$(d\Gamma/dE_e)_{corrected} = (d\Gamma^{(0)}/dE_e)F(\hat{x}) \tag{39}$$

with $\hat{x} = 2E_e/m_b$ and

$$F(\hat{x}) = [1 - \frac{2\alpha_s}{3\pi}G(\hat{x},0)]\exp[-\frac{2\alpha_s}{3\pi}\ln^2(1-\hat{x})]. \tag{40}$$

The radiative correction is taken from the work of Corbo[8] and the interested reader can find the function $G(\hat{x},0)$ in eq. (39) of ref. [8]. We note that the parton spectrum is lower and falls off less steeply than in the ACM model. Consequently, the values for V_{ub} extracted from the end-point energy will be *larger* in the parton model.

The double differential decay rate $d\Gamma/dE_e dM_X$ also depends strongly on the invariant mass of the hadrons M_X. We show in Fig. 7 $d\Gamma/dE_e dM_X$ for various values of M_X. The decay rate is larger in the range $0.2M_B \leq M_X \leq 0.4M_B$. The characteristic feature again is that the spectra shift to larger values of E_e as M_X decreases. After integration over M_X the sum of the curves give the mass distribution shown in figure 8. This agrees very closely with mass distributions published before[3] and is similar but not identical with the curves in ref. [9]. In Fig. 8, we also include the invariant mass spectrum for $b \to c$, to be discussed below.

For comparison we also calculated the distribution for the $B \to X_c + e^-\bar{\nu}$ decay. In Fig. 9 we show the double differential decay rate in E_e and q_0. Comparing with Fig. 4 we note that this channel runs out of events at $E_e = 2.25\ GeV$ and the events above $2\ GeV$ are very few. By making a cut in $q_0 > M_B - M_D = 0.65M_B$ there are no events left for $b \to c$. In Fig. 5 we showed two spectra ($b \to u$ and $b \to c$) for three values of ε_p. For these curves we have chosen $|V_{ub}| = |V_{cb}|$. It is clear that the $b \to c$ spectrum is softer and a very small fraction lies at $E_e > 2.0\ GeV$. Fig. 10 shows the distribution of events as a function of the invariant mass. For comparison we show in Fig. 8 the invariant mass distributions for the two decays together, taking $|V_{ub}| = |V_{cb}|$. The $b \to c$ decays peak in the region 1.8 to 2.2 GeV. That is, the parton model prefers that the hadrons produced fall within a hadronic mass where the D and D^* resonances occur and for this reason the constituent quarks can combine to form these resonances.

To date, only the inclusive endpoint electron spectrum has been used to extract evidence for $b \to u$ from semileptonic decay data. Additional cuts on the energy or invariant mass of the final hadronic system could be of great utility in probing the decay dynamics and separating $b \to u$ from $b \to c$ events. Such cuts could capture more $b \to u$ events and help to improve statistics on the important standard model parameter V_{ub}/V_{cb}.

5 SUMMARY AND CONCLUSIONS

The parton model provides an interesting alternative to the ACM model for analysing inclusive semileptonic decays in important kinematical regions where the decay is dominated by short distance physics. We have produced decay spectra for a variety of interesting and physically accessible observables which probe the decay dynamics in a much more complete way than the simple electron spectrum. These spectra are obtained from a simple and compact formula (eq. (35)) based a one parameter parton model. As high statistics data become available this model may play an increasingly important role in separating $b \to u$ from $b \to c$ decays and lead to a better determination of the V_{ub}/V_{cb}.

6 ACKNOWLEDGEMENTS

CHJ wishes to thank Deutscher Akademischer Austauschdienst (DAAD) for financial support. WFP wishes to thank the North Atlantic Treaty Organization for a Travel Grant. EAP wishes to acknowledge the hospitality of The Ohio State University, where this work was initiated.

References

[1] R. Fulton *et al.* (CLEO), *Phys. Rev. Lett.* **64** (1990) 16;
H. Albrecht *et al.* (ARGUS), *Phys. Lett.* **B234** (1990) 409;
D. Besson (CLEO Collaboration), Proceedings of the XVI International Symposium on Lepton-Photon Interactions, Cornell University, Ithaca, NY, August, 1993

[2] G. Altarelli, N. Cabibbo, G. Corbo, L. Maiani and G. Martinelli, *Nucl. Phys.* **B208** (1982) 365

[3] A. Bareiss and E.A. Paschos, *Nucl. Phys.* **B327** (1989) 353

[4] A. Bareiss, *Z. Phys.* **C53** (1992) 311

[5] S.J. Brodsky, C. Peterson and N. Sakai, *Phys. Rev.* **D23** (1981) 2745

[6] C. Peterson, D. Schlatter, J. Schmitt and P.M. Zerwas, *Phys. Rev.* **D27** (1983) 105

[7] J. Chrin, *Z. Phys.* **C36** (1987) 163

[8] G. Corbo, *Nucl. Phys.* **B212** (1983) 99

[9] V. Barger, C.S. Kim and R.J.N. Phillips, *Phys. Lett.* **B251** (1990) 629

Figure Captions

1. The semileptonic B-decay in the parton model (definition of kinematic variables).

2. The physical region in the q^2 vs E_e-plane for fixed values of $s = M_X^2$.

3. The physical region in the q_0 vs q^2-plane.

4. The $b \to u$ double differential decay rate $d\Gamma/dE_e dq_0$ vs E_e for various values of q_0 in the rest frame of the B meson. We set $m_u = 0, M_\pi = 0, M_B = 5.3\ GeV, \alpha_s = 0$ and $\varepsilon_p = 0.006$.

5. $d\Gamma/dE_e$ for semileptonic B meson decays in the rest frame of the B meson. The values for the parameters are $m_u = 0, m_c = 1.5\ GeV, M_B = 5.3\ GeV, M_D = 1.86\ GeV, \alpha_s = 0$ and various values of ε_p as shown.

6. The $b \to u$ spectrum in the ACM model and the parton model. Both curves include QCD radiative corrections with $\alpha_s = 0.24$.

7. The $b \to u$ double differential decay rate $d\Gamma/dE_e dM_X$ vs E_e for various values of M_X in the rest frame of the B meson. The values for the parameters are the same as in Fig. 4.

8. $d\Gamma/dM_X$ for semileptonic B meson decays in the rest frame of the B meson. The values for the parameters are $m_u = 0, m_c = 1.5\ GeV, M_B = 5.3\ GeV, M_D = 1.86\ GeV, \alpha_s = 0$ and $\varepsilon_p = 0.006$.

9. The $b \to c$ double differential decay rate $d\Gamma/dE_e dq_0$ vs E_e for various values of q_0 in the rest frame of the B meson. We set $m_c = 1.5\ GeV, M_B = 5.3\ GeV, M_D = 1.86\ GeV, \alpha_s = 0$ and $\varepsilon_p = 0.006$.

10. The $b \to c$ double differential decay rate $d\Gamma/dE_e dM_X$ vs E_e for various values of M_X in the rest frame of the B meson. The values for the parameters are the same as in Fig. 9.

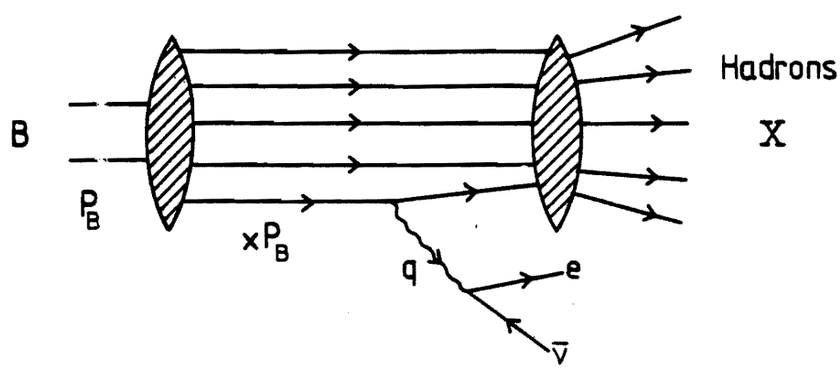

Fig. 1. The semileptonic B meson decay in the parton model.

Fig. 2

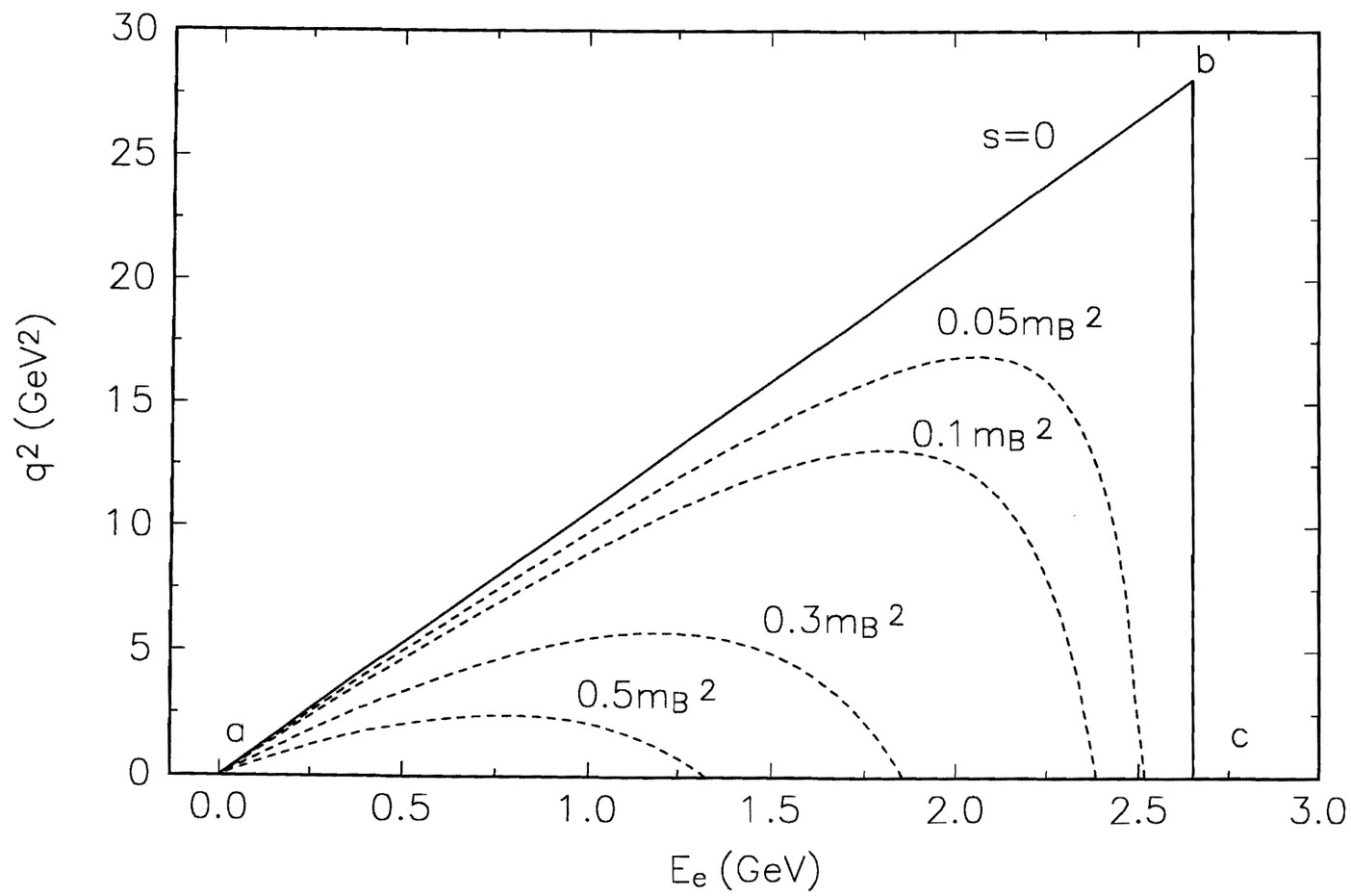
30
25
20
15
10
5
0
0.0
0.5
1.0
1.5
2.0
2.5
3.0
q2 (GeV2)
Ee (GeV)
s=0
0.05mB 2
0.1 mB 2
0.3mB 2
0.5mB 2
a
b
c

Fig. 3

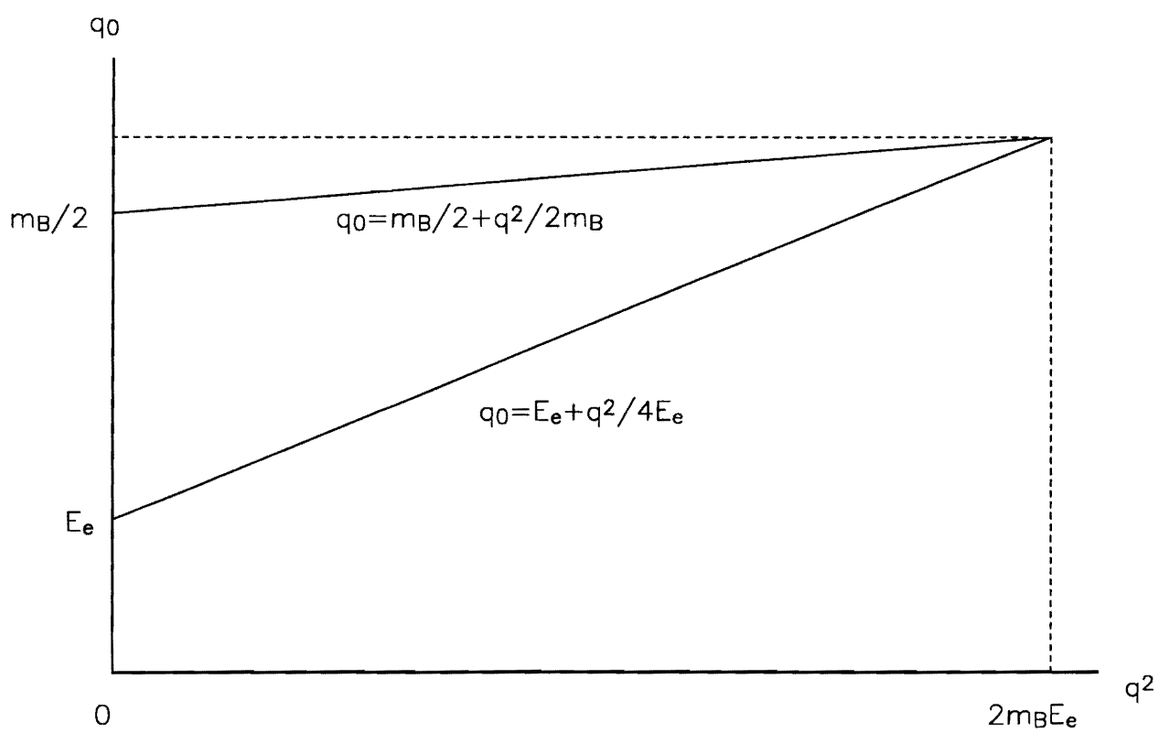

Fig. 4

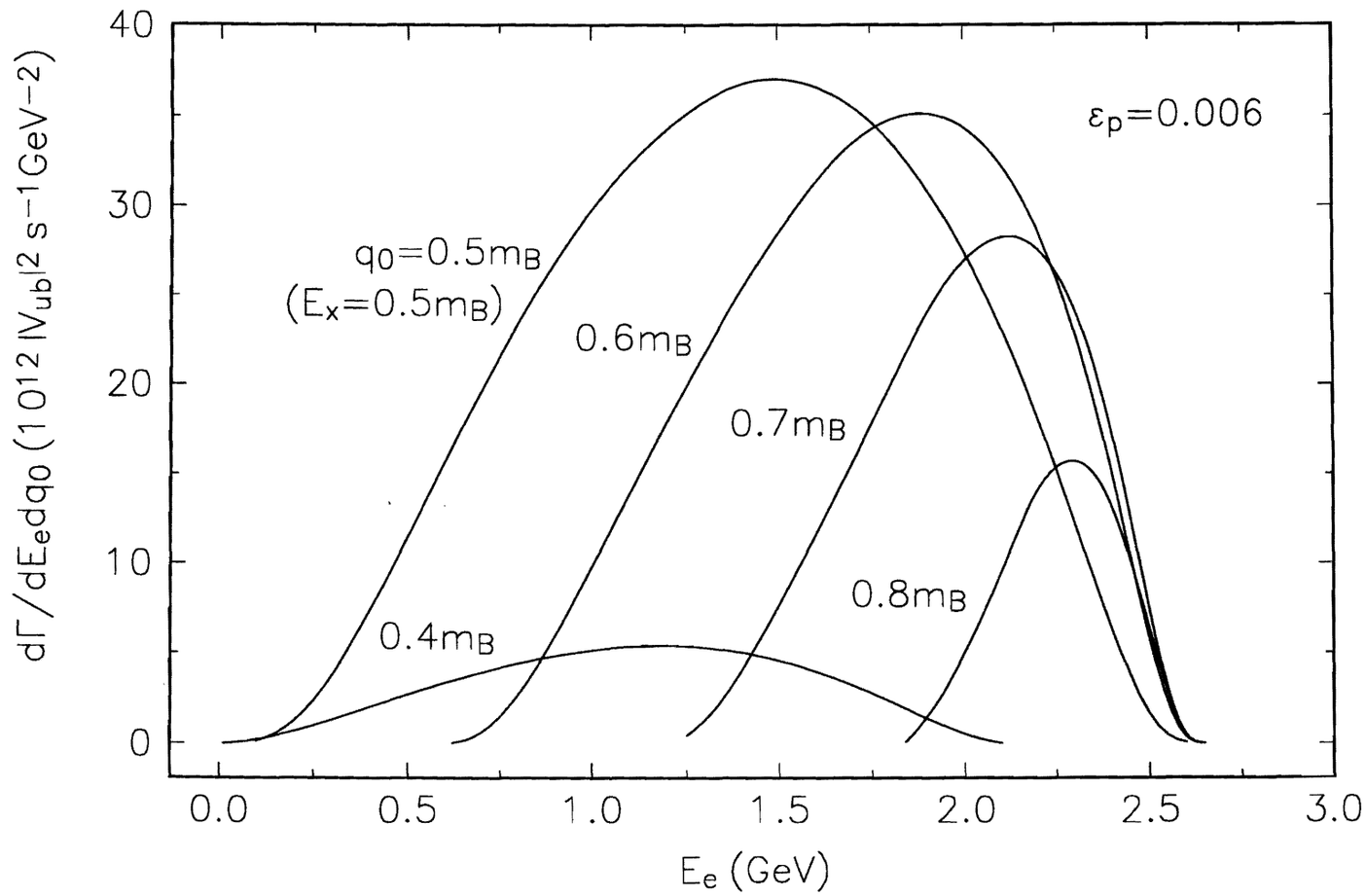
40
30
20
10
0
0.0
0.5
1.0
1.5
2.0
2.5
3.0
$d\Gamma/dE_e dq_0$ (10^{12} $|V_{ub}|^2$ s^{-1} GeV^{-2})
E_e (GeV)
ε_p=0.006
q_0=0.5m_B
(E_x=0.5m_B)
0.6m_B
0.7m_B
0.8m_B
0.4m_B

Fig. 5

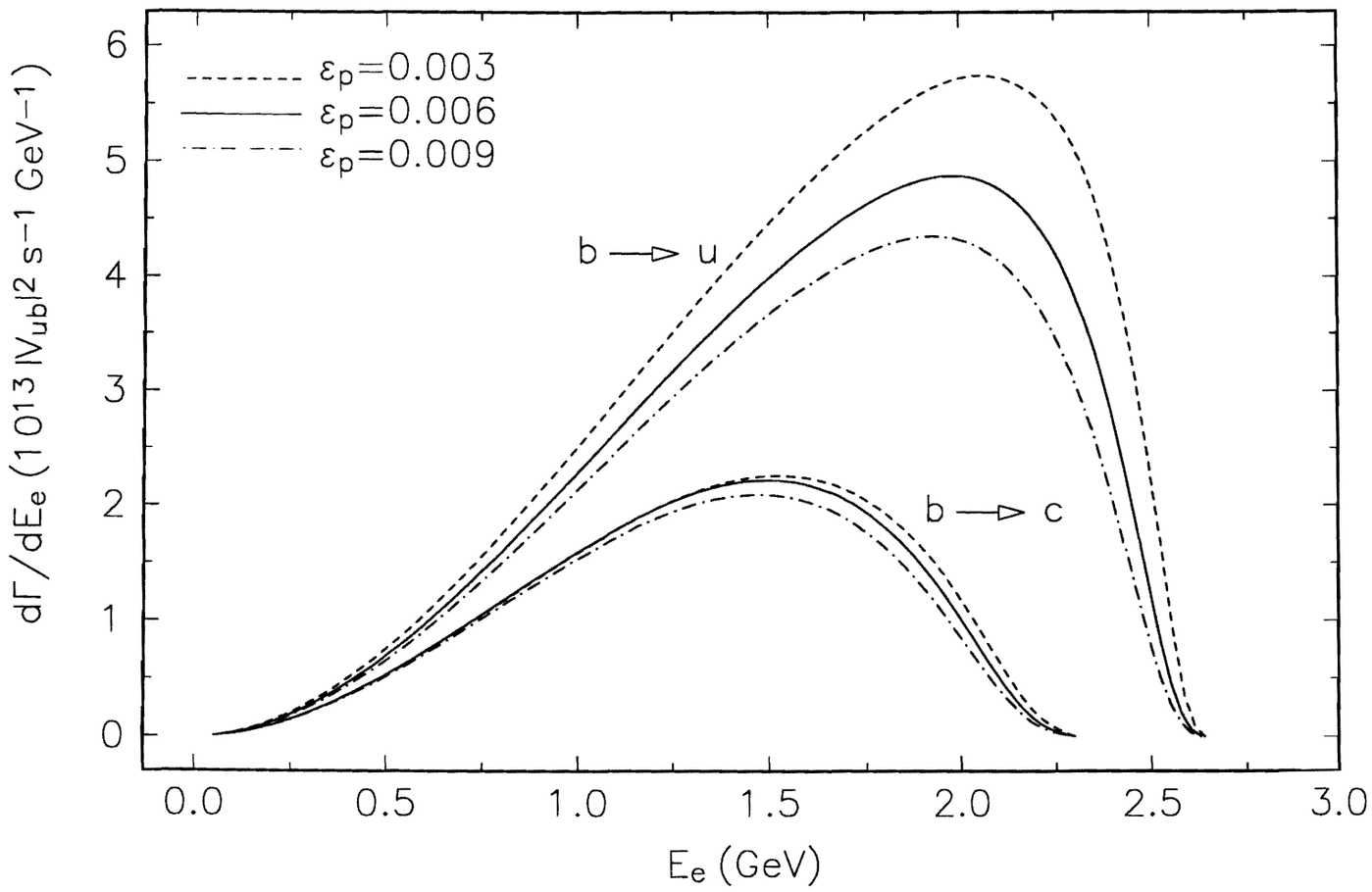
ε_p=0.003
ε_p=0.006
ε_p=0.009
b → u
b → c
$d\Gamma/dE_e$ (10^{13} $|V_{ub}|^2$ s^{-1} GeV^{-1})
E_e (GeV)
0
1
2
3
4
5
6
0.0
0.5
1.0
1.5
2.0
2.5
3.0

Fig. 6

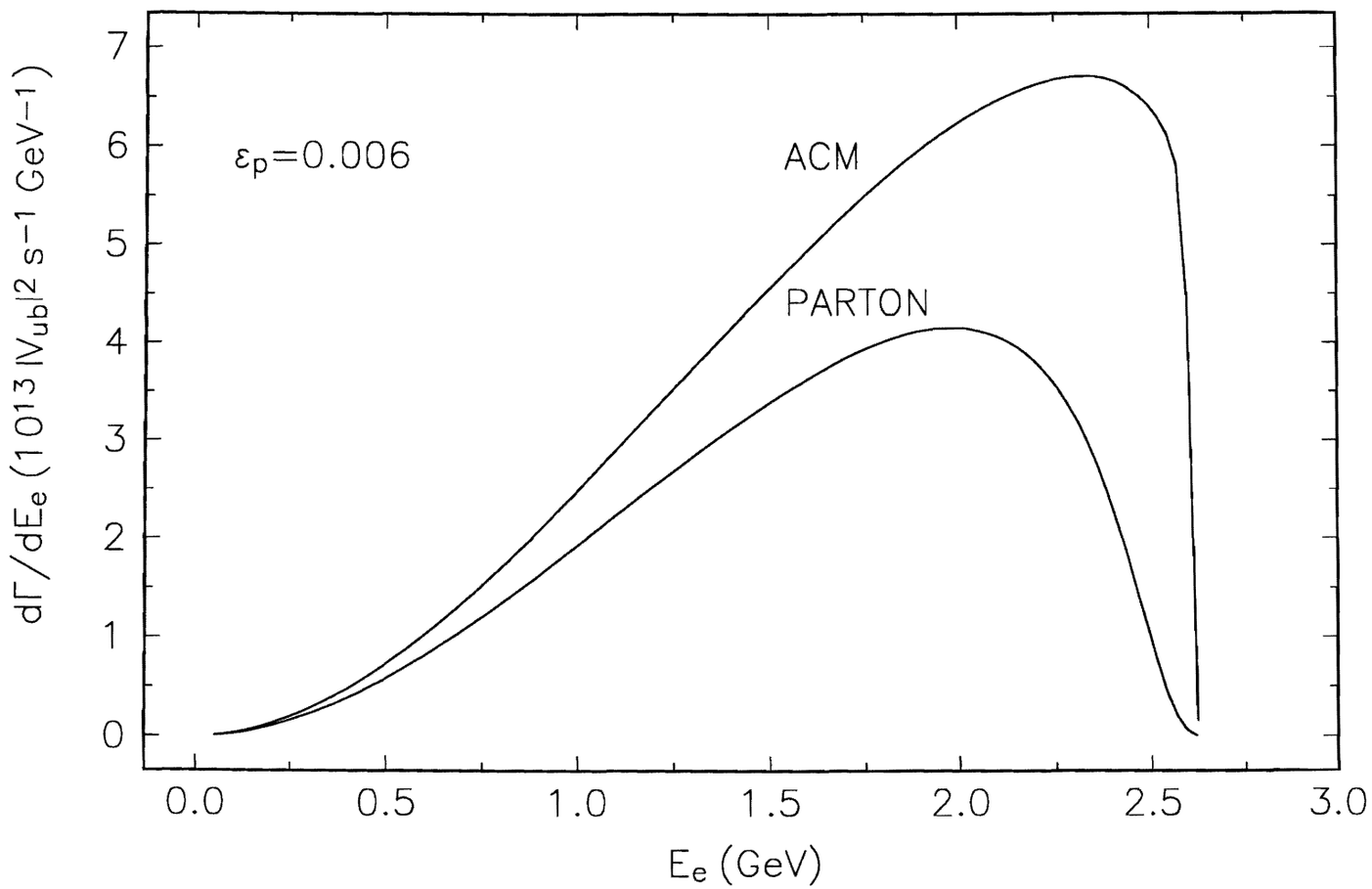
ε_p=0.006
ACM
PARTON
$d\Gamma/dE_e$ (10^{13} $|V_{ub}|^2$ s^{-1} GeV^{-1})
E_e (GeV)
0
1
2
3
4
5
6
7
0.0
0.5
1.0
1.5
2.0
2.5
3.0

Fig. 7

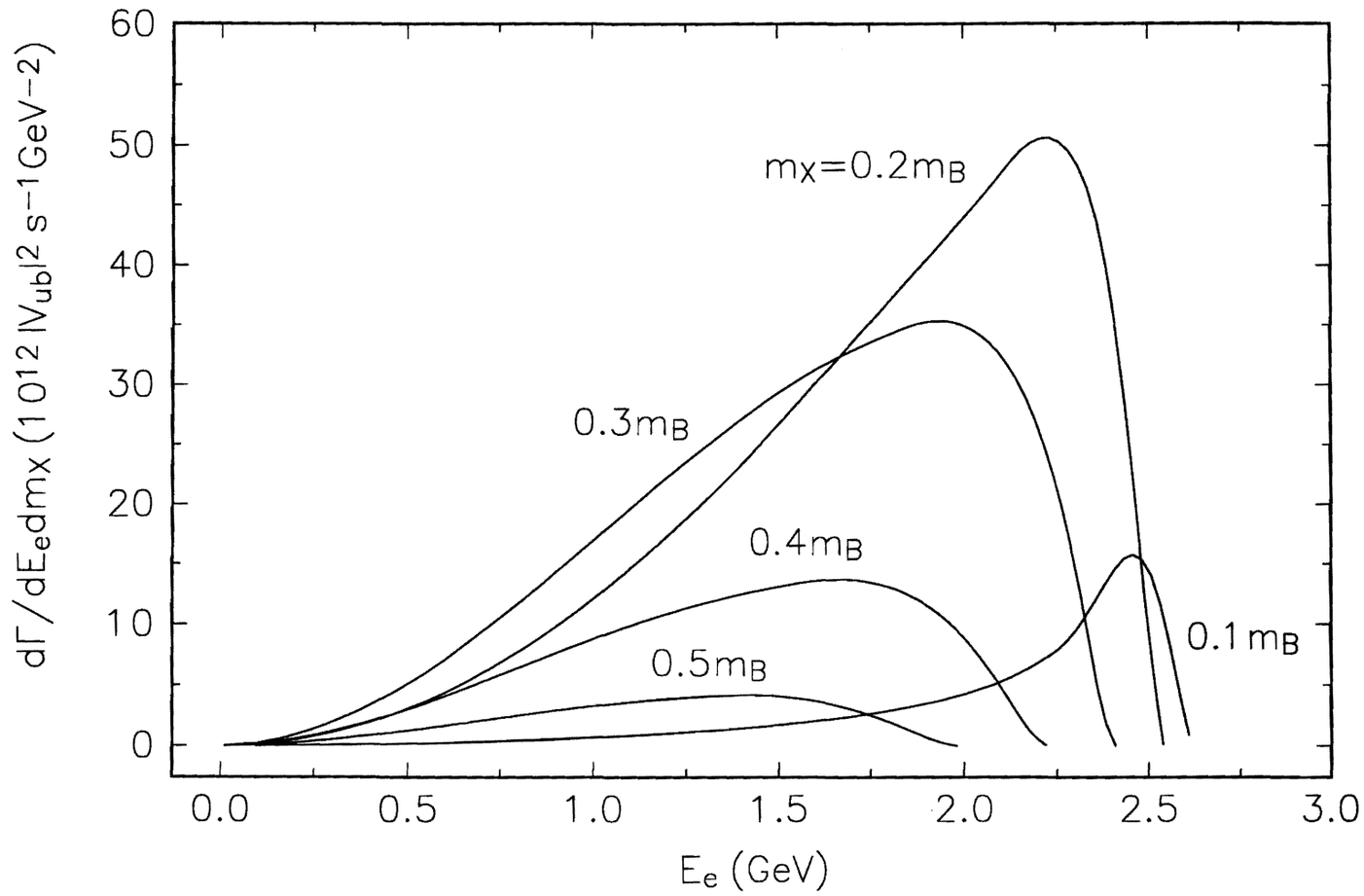
60
50
40
30
20
10
0
0.0
0.5
1.0
1.5
2.0
2.5
3.0
E_e (GeV)
$d\Gamma/dE_e dm_X$ (10^{12} $|V_{ub}|^2$ s^{-1}GeV^{-2})
m_X=0.2m_B
0.3m_B
0.4m_B
0.5m_B
0.1 m_B

Fig. 8

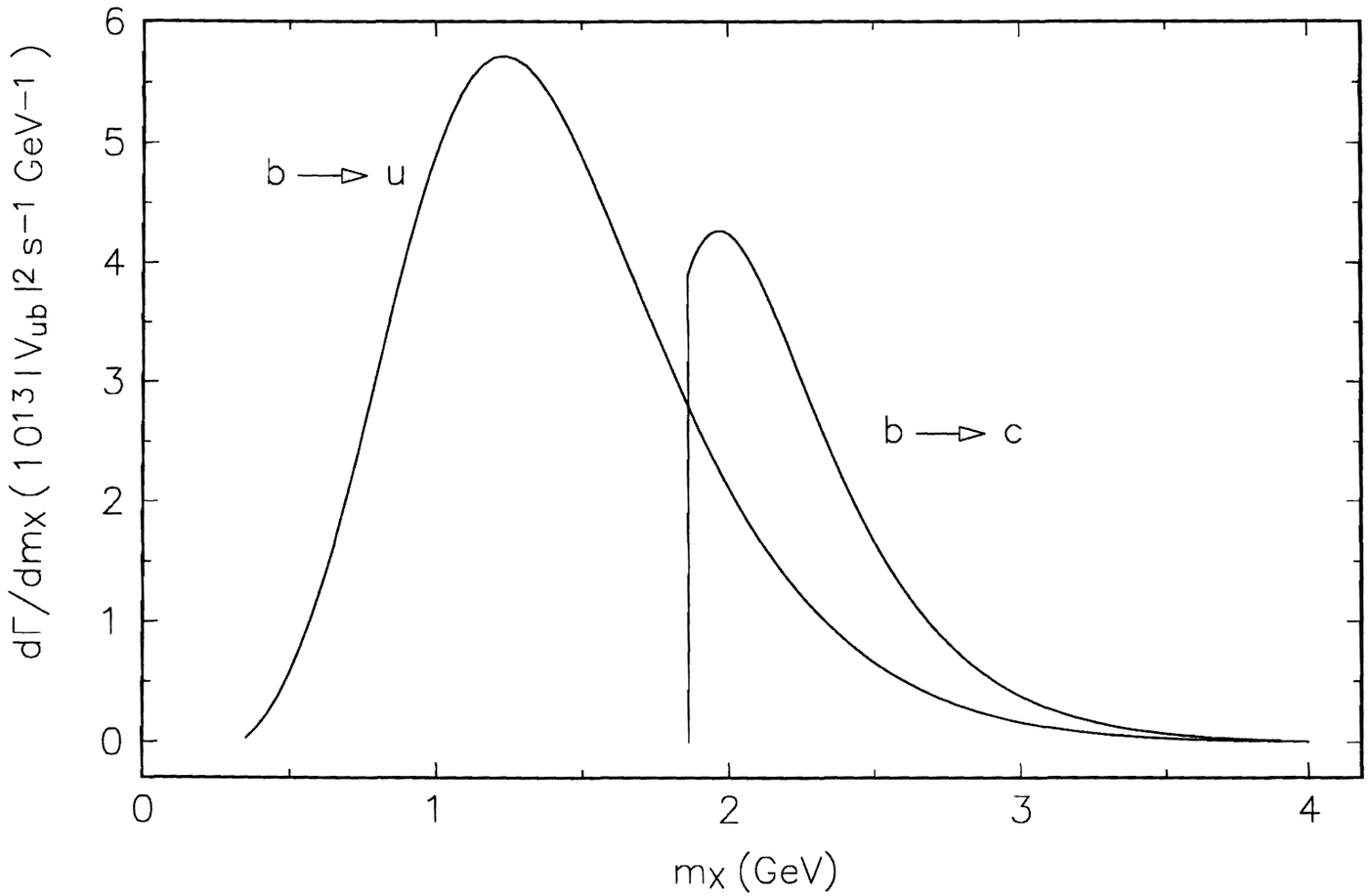

Fig. 9

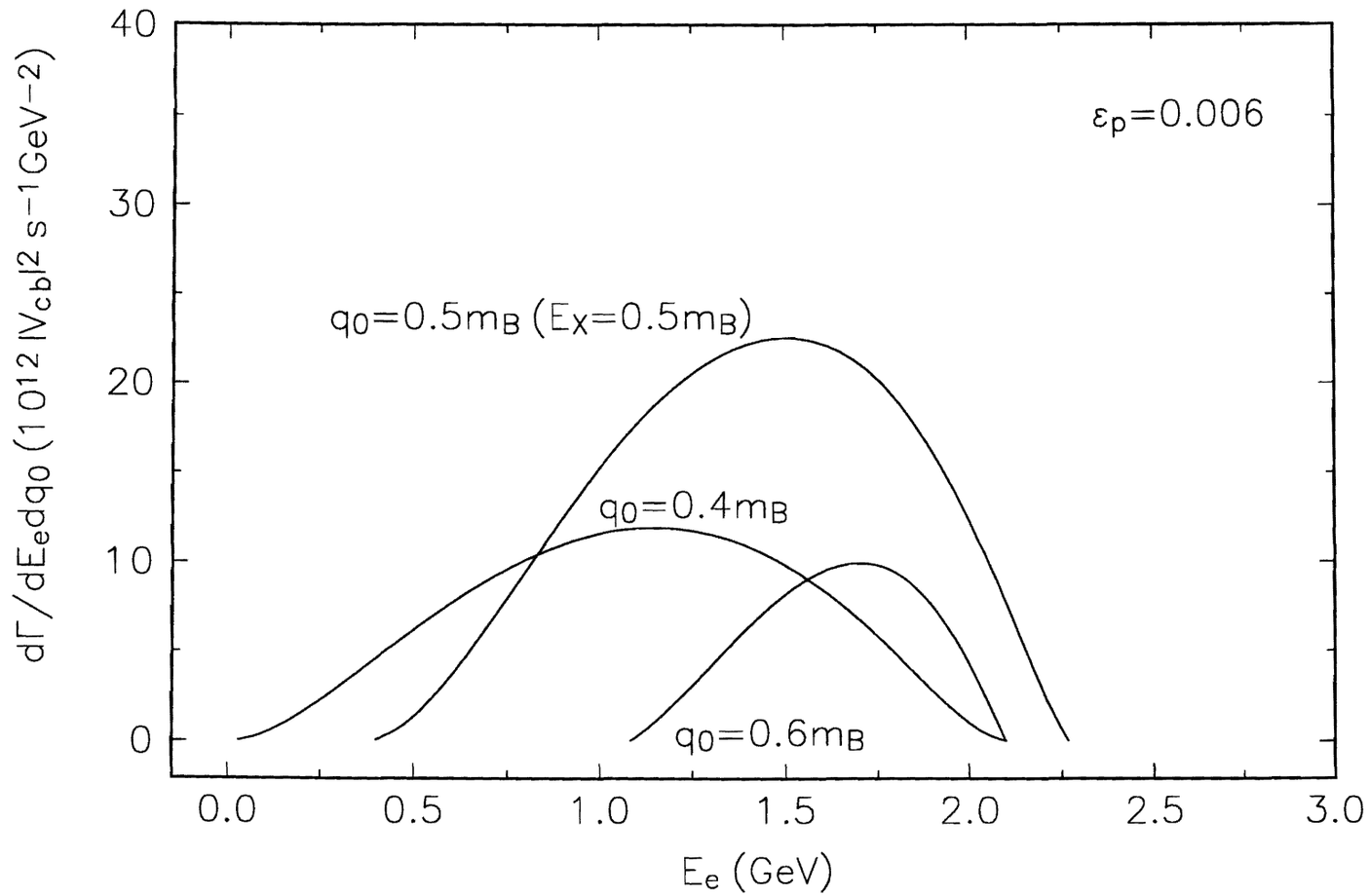
ε_p=0.006
q_0=0.5m_B (E_X=0.5m_B)
q_0=0.4m_B
q_0=0.6m_B
$d\Gamma/dE_e dq_0$ (10^{12} $|V_{cb}|^2$ s^{-1}GeV^{-2})
E_e (GeV)
0
10
20
30
40
0.0
0.5
1.0
1.5
2.0
2.5
3.0

Fig. 10

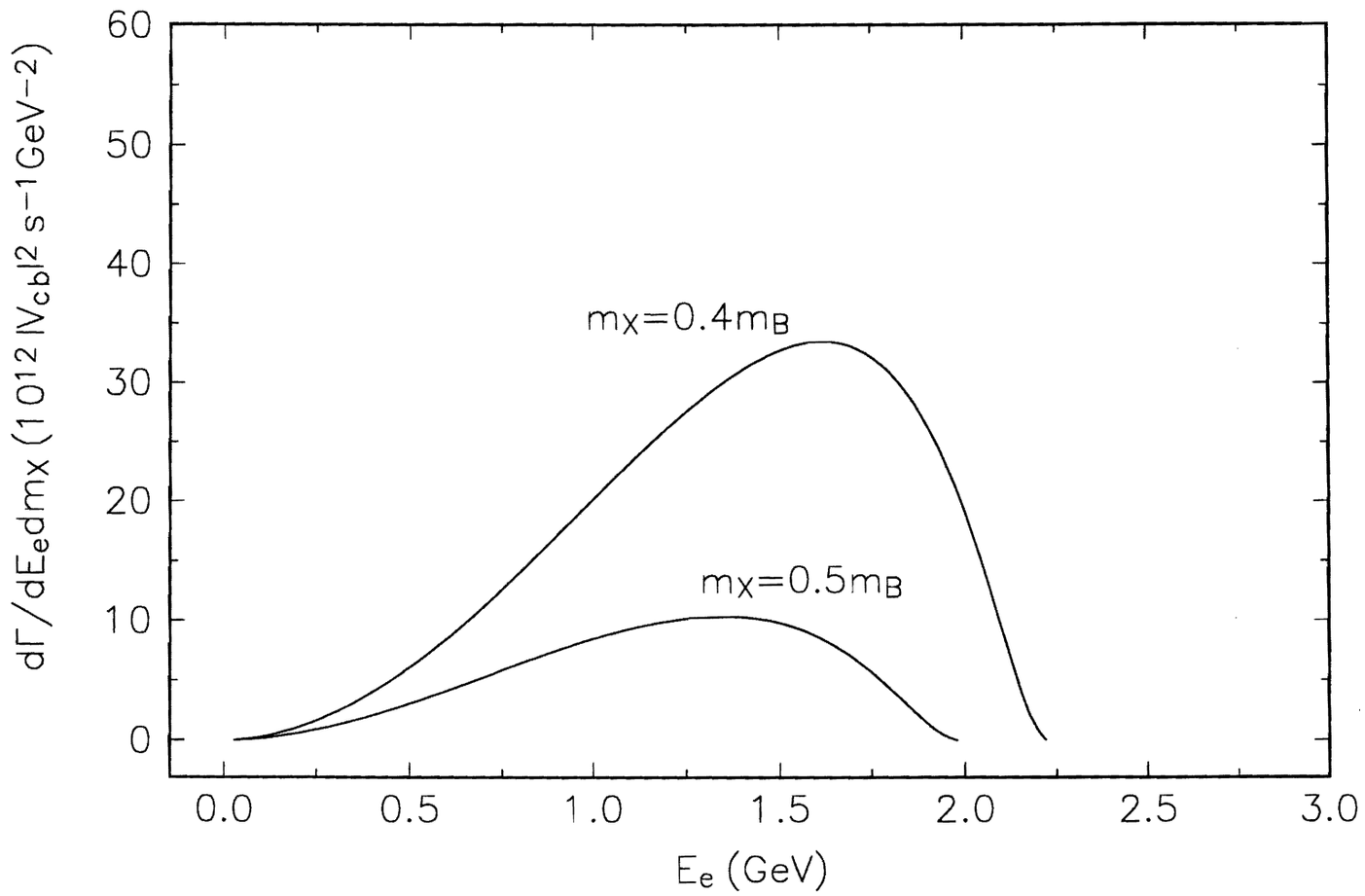
60
50
40
30
20
10
0
0.0
0.5
1.0
1.5
2.0
2.5
3.0
$d\Gamma/dE_e dm_X$ (10^{12} $|V_{cb}|^2$ s^{-1}GeV^{-2})
E_e (GeV)
m_X=0.4m_B
m_X=0.5m_B